CrossMark

ORIGINAL ARTICLE

Cerebral and blood correlates of reduced functional connectivity in mild cognitive impairment

Gabriel Gonzalez-Escamilla · Mercedes Atienza · David Garcia-Solis · Jose L. Cantero

Abstract Growing evidence suggests that decreased functional connectivity in cortical networks precedes clinical stages of Alzheimer's disease (AD), although our knowledge about cerebral and biological correlates of this phenomenon is limited. To shed light on this issue, we have investigated whether resting-state oscillatory connectivity patterns in healthy older (HO) and amnestic mild cognitive impairment (aMCI) subjects are related to anatomical grey matter (GM) and functional (2-[18F]fluoro-2-deoxy-D-glucose (FDG)-PET) changes of neuroelectric sources of alpha rhythms, and/or to changes in plasma amyloid-beta (Aβ) and serum lipid levels, blood markers tied to AD pathogenesis and aging-related cognitive decline. We found that aMCI subjects showed decreased levels of cortical connectivity, reduced FDG-PET intake of the precuneus, and GM atrophy of the thalamus, together with higher levels of Aβ and apolipoprotein B (ApoB) compared to HO. Interestingly, levels of high-density lipoprotein (HDL) cholesterol were positively correlated with the strength of neural-phase coupling in aMCI subjects, and increased triglycerides accompanied bilateral GM loss in the precuneus of aMCI subjects. Together, these findings provide peripheral blood correlates of reduced resting-state cortical connectivity in aMCI, supported by anatomo-functional changes in cerebral sources of alpha rhythms.

This framework constitutes an integrated approach to assess functional changes in cortical networks through neuroimaging and peripheral blood markers during early stages of neurodegeneration.

Introduction

Aging is characterized by morphological changes in neurons, synaptic loss, and alterations in neurotransmitter receptors (Masliah et al. 1993; Hof and Morrison 2004; Bishop et al. 2010). Aβ neuritic plaques and neurofibrillary tangles are also present in clinically intact older adults showing the same or different distribution as in Alzheimer's disease (AD) patients (Tomlinson et al. 1968; Katzman et al. 1988; Price et al. 1991), although age-related tangle formation does not by itself represent a process that would inevitably progress to AD (Price and Morris 1999). Therefore, the different degree of resistance to AD neuropathology (Snowdon 2003) together with the heterogeneity of clinical outcomes in individuals with comparable degrees of pathologic brain lesions (Iacono et al. 2009) illustrate the complexity of the aging process and foresees major obstacles to establish biological boundaries between normal aging and incipient neurodegeneration.

Synaptic dysfunctions and neuronal loss are two major pathological hallmarks of AD (DeKosky and Scheff 1990; Terry et al. 1991). Mounting evidence has shown that increased brain levels of soluble Aβ oligomers are linked to

G. Gonzalez-Escamilla · M. Atienza · J. L. Cantero (✉)
Laboratory of Functional Neuroscience, Spanish Network of Excellence for Research on Neurodegenerative Diseases (CIBERNED), Pablo de Olavide University, Ctra. de Utrera Km 1, 41013 Seville, Spain
e-mail: jlcanlor@upo.es

D. Garcia-Solis
Department of Nuclear Medicine, University Hospital Virgen del Rocio, Seville, Spain

synaptic damage in AD (Lambert et al. 1998; Mucke et al. 2000; Walsh et al. 2002; Lesné et al. 2006; Lacor et al. 2007), likely accounting for disruption of neural circuits (Hsia et al. 1999; Palop et al. 2007; Cao et al. 2012; Cheng et al. 2013) and aberrant connectivity patterns in distributed brain networks during disease progression (Babiloni et al. 2004; Greicius et al. 2004; Stam et al. 2006; Brier et al. 2012).

Alpha oscillations are intrinsically generated by pyramidal neurons of cortical layer 5 (Silva et al. 1991), which are affected by dense-core plaques in AD patients (Arnold et al. 1991). The thalamus, that also plays an important role in the generation of the alpha rhythm (Lopes da Silva 1991; Hughes et al. 2004), has shown modest Aβ deposits and neurofibrillary tangles in AD patients (Rudelli et al. 1984; Masliah et al. 1989; Braak and Braak 1991). However, it remains to be elucidated whether impaired functional connectivity of resting-state cortical networks is accompanied by anatomo-functional damage of cortical and thalamic sources of EEG-alpha rhythms in amnestic mild cognitive impairment (aMCI) subjects.

Up to now, neither Aβ nor lipid concentration in blood have been confirmed as reliable AD biomarkers. However, the plasma $A\beta_{1-42}/A\beta_{1-40}$ ratio predicts cognitive decline and AD progression (Koyama et al. 2012) as well as volume changes in the medial temporal lobe of healthy older (HO) subjects (Sun et al. 2011). Animal evidence also supports a link between alterations in lipid metabolism and AD pathogenesis (Pappolla et al. 2003; Shobab et al. 2005; Panza et al. 2006; Ghribi 2008; Martins et al. 2009; Di Paolo and Kim 2011), suggesting that elevated levels of cholesterol might contribute to accelerate AD progression (Simons et al. 1998; Grimm et al. 2008; Xiong et al. 2008) and to increase the risk for brain lesions and dementia (Leritz et al. 2011; Williams et al. 2013). However, no studies to date have investigated whether blood levels of Aβ and/or lipids are related to changes in the resting-state functional anatomy of the brain in aMCI subjects.

The purpose of the present study is therefore twofold: to investigate whether connectivity failures observed in aMCI are related to changes in grey matter (GM) and/or glucose consumption of the main neuroelectric sources of EEG-alpha rhythms; and to assess whether patterns of cortical connectivity are differently associated with changes in Aβ and lipid levels in HO and aMCI subjects.

Materials and methods

Subjects

Twenty-nine older adults with aMCI (10 females, mean age: 70.1 ± 6.8 years) and 26 HO subjects (15 females, mean age: 66.5 ± 4.9 years) were enrolled in the study. Participants were primarily recruited from older people's associations, normal community health screening, and hospital outpatient services. All of them gave written informed consent prior to experiments. Approval for the study was obtained from the Human Research Ethics Committee of the University Pablo de Olavide in accordance with the ethical standards of the Declaration of Helsinki.

Each participant underwent structured, uniform evaluation that included a medical history, neurological examination, and cognitive function testing. Only those who met established criteria (see below) were included in the study. Cerebral magnetic resonance imaging (MRI) was previously examined in all participants to rule out territorial cerebral infarctions, brain tumors, hippocampal sclerosis, and/or vascular malformations. Those subjects with large periventricular and/or deep white matter (WM) lesions, revealed by scores ≥2 on the Fazekas ischemic scale (Fazekas et al. 1987), were excluded from the study. Cardiovascular risk factors (hypertension, diabetes, overweight, family history of coronary heart disease or stroke) were also exclusion criteria.

aMCI subjects showed an idiopathic amnestic disorder with absence of impairment in cognitive areas other than memory, and they further met diagnostic criteria for aMCI (Petersen et al. 1999): (1) subjective memory complaints corroborated by the informant; (2) objective memory loss confirmed by the Spanish version of the Logical Memory subtest extracted from the Wechsler Memory Scale-Third Edition (WMS-III) (scorings 1.5 standard deviations below the age-appropriate mean); (3) global score of 0.5 (questionable dementia) in the clinical dementia rating (CDR); (4) normal independence function; and (5) no DSM-IV criteria for dementia. The global cognitive status was assessed with the Mini Mental State Examination (MMSE), adapted and validated for Spanish population (Blesa et al. 2001). A neurologist with long-standing experience in the diagnosis and treatment of dementia made the diagnosis of aMCI and ruled out any medical or neurological conditions in HO subjects. The diagnosis was further supported by results derived from a comprehensive neuropsychological battery: Boston Naming Test, Trail Making Test, Rey-Osterrieth Complex Figure Test, Visual Object and Space Perception Battery, verbal fluency and word list (Wechsler Memory Scale). The absence of secondary causes of cognitive deficits was confirmed by laboratory tests including complete blood count, vitamin B12/folate, and thyroid function tests. Elderly depression was excluded using the shorter version of the Geriatric Depression Scale (Yesavage et al. 1983). None of the participants were taking cholinesterase inhibitors, and/or psychiatric medication at the time of recruiting or during the study.

Inclusion criteria for HO subjects were (1) absence of cognitive impairment (memory, language, attention, and

executive function) confirmed by neuropsychological assessment, (2) CDR global score of 0 (no dementia), and (3) normal independent function. HO subjects were tested following the same neuropsychological protocol as for aMCI subjects.

APOE genotyping

Genomic DNA was isolated from blood using a salting-out protocol (Miller et al. 1988), and ApoE polymorphisms were determined with pre-designed TaqMan SNP geno-typing assays (Applied Biosystem). The presence/absence of the ApoE ε4 allele was not employed as an inclusion criterion during the recruiting process.

Blood Aβ and lipid levels

Venous blood samples were obtained after overnight fasting. Blood samples were collected in 10 mL K2-ethyle-nediaminetetraacetic acid (EDTA) coated tubes (BD Diagnostics), and further centrifuged (3,500 rpm) at 4 °C for 5 min. Supernatant plasma was collected and aliquoted into 250-μL polypropylene tubes containing 8.32 μL of a protease inhibitor cocktail (cOmplete Ultra Tablets mini, Roche). Plasma samples were stored at −80 °C and thawed immediately before assay.

Plasma Aβ levels were measured blind to cognitive status in duplicate samples (50 μL) according to manufacturer's instructions (Invitrogen). Averaged values (pg/ml) were used for statistical analyses. Human $A\beta_{1-40}$ and ultra sensitive $A\beta_{1-42}$ specific enzyme-linked immunoassay (ELISA) kits were used for this purpose. The detection limit of these assays was 0.52 pg/ml for $A\beta_{1-40}$ and 0.27 pg/ml for $A\beta_{1-42}$. Both inter-assay and intra-assay coefficients of variation were below 10 %. The $A\beta_{1-42}/A\beta_{1-40}$ ratio was additionally computed for each subject given its ability to identify cognitively normal subjects who are at increased risk of developing MCI or AD (Graff-Radford et al. 2007), and its association with cognitive decline (Koyama et al. 2012) and with volume loss of the medial temporal lobe in HO adults (Sun et al. 2011).

Fasting serum levels of total cholesterol (TCh), low-density lipoprotein (LDL), high-density lipoprotein (HDL), triglycerides (TRIG), and apolipoprotein B (ApoB) were obtained in each participant with the automated A15 Random Access Analyzer® (Biosystems S.A., Barcelona, Spain) using Biosystems commercial test kits.

EEG recordings and signal preprocessing

EEG recordings were obtained from 59 scalp electrodes referenced to linked-mastoids, and positioned according to the extended International 10–10 system. Additional electrodes were placed for monitoring vertical–horizontal eye movements and the muscular tone. Continuous EEG recordings were performed in resting state with eyes closed for 10 min between 9 and 10 AM. Electrophysiological measurements were amplified (BrainAmp MR, Brain Vision®), filtered (0.1–100 Hz bandpass), digitized (250 Hz, 16-bit resolution), and stored in digital format for subsequent analyses.

EEG epochs were transformed into the common average reference to partially avoid pernicious effects of reference on neural-phase synchrony results (Schiff 2005). Ocular and muscle artifacts were removed by applying Independent Component Analysis (Infomax algorithm), as implemented in the BrainVision Analyzer software v. 1.05 (Brain Products® GmbH). Epochs with noisy EEG channels were manually selected and excluded from further analysis to avoid artificial coupling patterns across electrodes. Quality of EEG recordings was apparently similar in HO and aMCI subjects precluding group effects in functional connectivity due to this factor.

Artifact-free EEG epochs from each participant were filtered within the alpha band (7.5–12.5 Hz), and the alpha peak frequency, defined as the maximum value of spectral power within the alpha band, was computed for each subject. Finally, artifact-free EEG epochs were bandpass filtered within the alpha peak frequency ±0.5 Hz (Kaiser window, filter order: 1326th, frequency attenuation: 0.5 Hz).

Determining neural-phase coupling in resting-state cortical networks

We calculated instantaneous phases with the Hilbert transform. Neural-phase coupling between pair-wise combinations of scalp EEG signals was computed using the phase lag index (PLI, Stam et al. 2007):

$$PLI = |< sign[\Delta\varphi(t_k)] >|$$

where $\Delta\varphi(t_k)$ represents the phase difference between the two EEG signals in the time sample t_k. The PLI quantifies how consistently one EEG signal is phase leading or lagging another EEG signal across time, disregarding zero-lag phase differences mainly due to volume conduction and/or active reference electrodes. PLI values range from 0 (no phase coupling) to 1 (perfect phase locking). The first 7 artifact-free EEG epochs of 8-s length were automatically selected in each participant. For each pair of scalp EEG electrodes and subject, we obtained a PLI value that resulted from averaging PLIs computed for each of the artifact-free EEG epochs. The same procedure was applied to surrogate data (see below).

To obtain functional connectivity patterns between EEG signals in each group, electrodes were previously grouped into four regions of interest (ROIs) for the left hemisphere

(frontal ROI: F7, F5, F3, F1, FC5, FC3, FC1; temporal ROI: FT7, T7, TP7; parietal ROI: Cp5, CP3, Cp1, P7, P5, P3, P1; and occipital ROI: PO7, PO3, O1) and their homologous ROIs for the right hemisphere. Electrodes placed in the midline were removed from further analyses together with other EEG locations commonly affected by muscular and oculomotor artifacts. PLIs were computed within each ROI as well as between ROIs, for the same hemisphere or between left and right hemispheres. Overall, we computed 780 PLIs for each subject: 380 PLIs within the same hemisphere and 400 PLIs between different hemispheres.

Cerebral MRI acquisition and image preprocessing

Structural cerebral images were acquired on a whole-body Philips Achieva 3T MRI scanner, using an 8-channel head array coil. A high-resolution MP-RAGE (magnetization-prepared rapid gradient echo) T1-weighted cerebral scan was obtained in each participant. Acquisition parameters were empirically optimized for GM/WM contrast (repetition-time = 2,300 ms, echo-time = 4.5 ms, flip angle = 88, matrix dimensions 256 × 192, 184 contiguous sagittal 1.2 mm thick slices, time per acquisition = 5.4 min).

Cerebral MRIs were visually inspected for artifacts (e.g., excessive blurring due to head motion, poor GM/WM contrast), and those brain scans with poor quality were repeated within the same week. Structural brain images were processed and analyzed with an optimized voxel-based morphometry (VBM) procedure implemented in SPM8 (www.fil.ion.ucl.ac.uk/spm). Briefly, T1 cerebral images on native space were partitioned into GM, WM and cerebrospinal fluid (CSF). GM and WM maps were then registered to the Montreal Neurological Institute canonical brain (MNI152) using DARTEL, a fast diffeomorphic image registration algorithm that minimizes anatomical variations among subjects preserving topology (Ashburner 2007). Resultant cerebral images were resampled to 1.5 mm^3 isotropic voxel size. To maintain total GM within the normalized compartments, GM maps were multiplied by relative volumes of warped and unwarped structures derived from the non-linear step of spatial normalization (Jacobian determinants) (Ashburner and Friston 2000). Resultant non-linear modulated warped GM maps were finally smoothed with an isotropic Gaussian kernel of 16 mm.

FDG-PET acquisition and image preprocessing

FDG-PET cerebral images were acquired on a whole-body PET-TAC Siemens Biograph 16 HiREZ scanner (Siemens Medical Systems, Germany) with in-plane and axial resolution of 4.2 and 4.5 mm full-width at half maximum (FWHM), respectively. Subjects fasted for at least 8 h before PET examination. Intravenous lines were placed 10–15 min before tracer injection of a mean dose of 370 MBq of 2-[18F]fluoro-2-deoxy-D-glucose (FDG). Participants stayed in a dimly lit room with their eyes closed to minimize external stimuli during the FDG uptake period. PET scans lasted approximately 30 min. A transmission scan was used for attenuation correction, and FDG-PET cerebral images were reconstructed with 2.6 × 2.6 × 2 mm voxel resolution using standard 2D back-projection filters. We applied partial volume correction (PVC) to cerebral FDG-PET cerebral images with the algorithm implemented in the PMOD software v3.17 (http://www.pmod.com) (Giovacchini et al. 2004).

Absolute values of PVC-FDG cerebral images were normalized to the mean cerebellar glucose consumption using the native brain space of each participant. Next, individual PVC-FDG images normalized to the cerebellum were registered with DARTEL to the MNI152 brain space by applying normalization parameters (deformation fields) previously obtained for cerebral MRI. Modulated warped maps of cerebral glucose consumption were finally smoothed with an isotropic Gaussian kernel of 16 mm.

Obtaining anatomical masks of cerebral sources of EEG-alpha rhythm

Evidence suggests that neuroelectric sources of the human alpha rhythm are located in the cuneus (occipital cortex), precuneus (superior parietal lobe) and thalamus (Cantero et al. 2009a, b). Therefore, all VBM analyses (MRI and FDG-PET) performed in the current study were limited to these ROIs.

Anatomical delimitation of EEG-alpha cerebral sources was obtained with the automated segmentation method implemented in Freesurfer v5.1 (https://surfer.nmr.mgh.harvard.edu/). First, manual edits were introduced in individual brain segmentations until the output was deemed acceptable upon visual inspection. Next, anatomical volume masks of EEG-alpha cerebral sources obtained from each subject were transformed into the same spherical coordinate system and further resampled to the spherical average surface of the study population (Fischl et al. 1999a, b). A transformation matrix was computed to convert average space coordinates of previously segmented alpha cerebral sources into the MNI152 brain space (resampled to 1.5 mm^3 isotropic voxel size), allowing us to perform voxel-wise group analysis with anatomo-functional (GM and glucose consumption) masks of EEG-alpha cerebral sources in the same brain space.

Statistical analyses

We previously assessed the normality assumption of data distribution with the Kolmogorov–Smirnov test. All

demographics, cognitive, and plasma Aβ/serum lipid values were normally distributed, allowing us to apply parametric statistical tests.

Group differences in demographic and cognitive variables were assessed with unpaired t tests, whereas the influence of gender and ApoE ε4 was tested with the Chi-square test due to the categorical nature of these variables. Group differences in blood Aβ ($A\beta_{1-40}$, $A\beta_{1-42}$, $A\beta_{1-42}$/$A\beta_{1-40}$ ratio) and lipid levels (TCh, LDL, HDL, TRIG, ApoB) were assessed using different analyses of covariance (ANCOVA) adjusted for age and gender. All these analyses were performed with SPSS v. 15 (SPSS Inc. Chicago, IL).

A bootstrap method was employed to determine if PLI values were significantly above noise and, consequently, had physiological meaning (Lachaux et al. 1999). For each pair of scalp EEG signals, we generated 2,000 surrogate data by adding a temporal shift (a random lag between 4 and 8 s) in one of the two EEG signals originally used to compute the PLI. Surrogate data was then used to compute distribution of 2,000 PLI values for each pair of EEG signals. The PLI value corresponding to the 95th quantile of the surrogate distribution was chosen as the significance threshold. Original PLIs obtained in each group were compared to the thresholded surrogate-PLIs using the Wilcoxon–Mann–Whitney test (Pereda et al. 2005). Only those PLIs that reached statistical significance ($p < 0.05$) in at least one of the two groups (HO and/or aMCI; aMCI ε4 carriers and/or non-carriers) were selected for further analyses.

Next, we determined group differences for each significant PLI. To aim this goal, significant PLIs were permutated by randomly assigning a number of HO subjects to the aMCI group. We computed the T^2 statistic on each permutation ($n = 2,000$) using the maximum squared T statistic ($\max T^2$) for each PLI, and the 95th quantile of this $\max T^2$ distribution as statistical threshold . This procedure is aimed at controlling the family-wise error (FWE) rate for all pairs of electrodes jointly (Maris 2004). Only those PLI values that reached significant group differences ($p < 0.05$, FWE corrected) were reported in the current study, and they were next used for correlations with GM volume and glucose consumption of cerebral sources of alpha rhythms.

Group differences in GM volume/glucose consumption of alpha cerebral sources (cuneus, precuneus, and thalamus) were assessed using the modulated VBM approach implemented in SPM8 (ANCOVA with age, gender, and either GM volume or glucose consumption of alpha cerebral sources as covariates, $p < 0.05$ FWE corrected).

Voxel-wise linear regression analyses were performed to test for relationships between anatomical (GM)/functional (FDG-PET) changes in neural sources of EEG-alpha rhythms and patterns of resting-state EEG coupling. These analyses included group (HO versus aMCI; aMCI ε4 carriers versus non-carriers), age, gender, GM volume/glucose consumption of alpha cerebral sources, and PLI as regressors. Regression analyses were separately performed for each significant PLI (Z-score transformed). PLIs were split into two groups to test for group differences (T-contrasts) in the way that PLI changes correlated with variations in GM volume/glucose consumption of alpha cerebral sources ($p < 0.05$, FWE corrected). Regression slopes were compared when correlations reached statistical significance in at least one of the two groups. A similar statistical approach was employed to study relationships between GM volume/glucose consumption of alpha cerebral sources and plasma Aβ/serum lipid levels.

Further regression analyses were performed to test for associations between plasma Aβ/serum lipid levels and patterns of resting-state cortical connectivity. If at least one of the two groups reached significance, differences between regression slopes were further assessed. These regression analyses were also adjusted for age and gender.

Results

Demographics, cognitive profile, and ApoE4 genotype

Table 1 includes demographic characteristics and cognitive profile for each group. As expected, subjects with aMCI showed significantly lower scores in MMSE ($p < 0.01$), immediate ($p < 10^{-6}$) and delayed verbal memory ($p < 10^{-10}$) than the HO individuals. The ApoE4 genotype was approximately fourfold higher in aMCI (48.3 %) than in HO subjects (11.5 %). The ε2/ε4 polymorphism was present in only one aMCI subject. aMCI ApoE4 carriers and non-carriers showed similar demographic and cognitive profiles, with the exception of impaired immediate memory ($p < 0.03$) and a trend toward significance in delayed recall of aMCI ApoE4 carriers ($p < 0.07$).

Group differences in Aβ and lipid levels

Table 2 shows mean values of plasma Aβ and serum lipid levels for each group. Overall, Aβ levels significantly differed between the two groups ($F_{3,49} = 5.2$, $p = 0.003$). Post hoc analyses revealed that aMCI showed higher concentrations of $A\beta_{1-40}$ ($p = 0.01$) and $A\beta_{1-42}$ ($p = 0.001$) than HO subjects, whereas group differences in the $A\beta_{1-42}$/$A\beta_{1-40}$ ratio did not reach significance.

The MANCOVA revealed that serum lipid levels were significantly different between the two groups ($F_{5,47} = 2.48$, $p < 0.04$), although only ApoB showed significant increased levels in aMCI compared to HO subjects ($p = 0.05$). aMCI ApoE4 carriers and non-carriers

Table 1 Demographics, cognitive profile, and ApoE ε4 distribution

	HO	aMCI	$p<$	aMCI ε4$^-$	aMCI ε4$^+$	P
Age (years)	66.5 ± 4.9	70.2 ± 6.8	0.08	68.6 ± 7.1	71.8 ± 6.2	0.2
Gender (F/M)	15/11	10/19	0.09	3/12	7/7	0.09
Education (years)	8.6 ± 4.3	8.2 ± 5.4	0.8	7.7 ± 5.2	8.8 ± 5.7	0.6
CDR (sum of boxes)	0	0.5	N/A	0.5	0.5	N/A
MMSE	28.3 ± 1.3	26.8 ± 2.6	0.01*	27.5 ± 2.6	26.0 ± 2.5	0.1
Immediate recall	14.2 ± 3.1	9.2 ± 2.9	10^{-6}*	10.3 ± 2.7	8.0 ± 2.7	0.03*
Delayed recall	13.2 ± 2.9	5.6 ± 3.7	10^{-10}*	6.8 ± 3.9	4.3 ± 3.2	0.07
TMT						
TMT-A (s)	49.7 ± 27	53.4 ± 33	0.7	50.1 ± 21	55.2 ± 30	0.7
TMT-B (s)	109 ± 46	125 ± 51.5	0.5	120 ± 11	129 ± 29	0.6
VOSP						
Screening	20	19.9 ± 0.2	0.9	19.6 ± 0.1	19.8 ± 0.4	0.9
Incomplete letters	19.4 ± 0.6	19.3 ± 0.9	0.9	19 ± 0.5	19.6 ± 0.6	0.7
Silhouettes	19.4 ± 0.6	17.5 ± 4.6	0.4	18.5 ± 1.3	19.5 ± 3.8	0.5
Object decision	15.5 ± 2.6	13.8 ± 6	0.5	14.8 ± 2.1	15.8 ± 2.5	0.3
Progress. silhouettes	11.71 ± 2.4	10.3 ± 8.1	0.8	10.9 ± 3.1	9.7 ± 2.8	0.4
Dot counting	9.9 ± 0.7	9.9 ± 0.2	0.9	9.7 ± 0.1	9.8 ± 0.1	0.8
Posit. discrimination	19.7 ± 1.8	18.6 ± 2	0.6	18.9 ± 0.5	18.3 ± 0.8	0.8
Number location	8.69 ± 1.6	8.3 ± 1.6	0.8	8.1 ± 2.1	8.5 ± 0.9	0.6
Cube analysis	8.6 ± 1.9	7.2 ± 2.7	0.2	7.6 ± 1.8	6.9 ± 2.3	0.4

Results are expressed as mean ± standard deviation

CDR clinical dementia rating, CDR = 0 no dementia, CDR = 0.5 questionable or very mild dementia. *MMSE* mini-mental state examination; *TMT* Trail Making Test, forms A and B; *VOSP* Visual object and space perception battery; *F/M* female/male; *ε4$^-$* ApoE ε4 non-carriers; *ε4$^+$* ApoE ε4 carriers

P exact *p* value. Significant *P* values were marked with an asterisk. N/A (not applicable)

Table 2 Aβ and serum lipid levels

Biological markers	HO	aMCI	P
Aβ$_{1-40}$ (pg/ml)	60.5 ± 5.4	80.6 ± 6.1	0.01*
Aβ$_{1-42}$ (pg/ml)	3.8 ± 0.3	5.9 ± 0.5	0.001*
Aβ$_{1-42}$/Aβ$_{1-40}$	0.08 ± 0.01	0.07 ± 0.006	0.7
Total cholesterol (mg/dL)	202.3 ± 7.4	210.1 ± 7.5	0.5
LDL cholesterol (mg/dL)	112.3 ± 5.9	112.5 ± 5.7	0.9
HDL cholesterol (mg/dL)	49 ± 2.6	46.9 ± 2.4	0.9
Triglycerides (mg/dL)	121.9 ± 8.5	123 ± 8.2	0.9
ApoB (mg/dL)	110.3 ± 4.1	126 ± 7.8	0.050*

Results are expressed as mean ± standard error of the mean

Aβ amyloid-beta, *LDL* low-density lipoprotein, *HDL* high-density lipoprotein, *ApoB* Apolipoprotein B

P exact *p* value of post hoc analysis, after significant MANCOVA. Significant *P* values were marked with an asterisk

did not show significant differences either in plasma Aβ or serum lipid levels.

Group differences in resting-state alpha-phase coupling

Figure 1 illustrates differences in alpha-phase coupling between HO and aMCI subjects (left column), and between aMCI ApoE4 carriers and non-carriers (right column). The
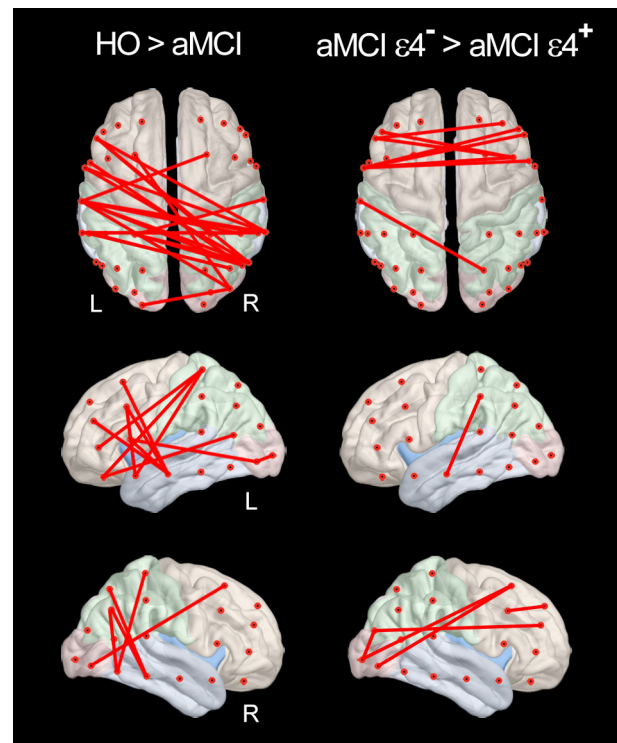

Fig. 1 Group differences in alpha-phase coupling between HO and aMCI subjects (*left column*), and between aMCI ApoE4 carriers and non-carriers (*right column*). *L* left hemisphere; *R* right hemisphere

Table 3 Group differences in GM and glucose consumption of EEG-alpha generators

EEG-alpha source	CS	x	y	z	T_{49}	P
GM (HO > aMCI)						
R thalamus	1,603	21	−16	−5	5.20	0.001
L thalamus	471	−23	−22	−5	5.31	0.001
FDG-PET (HO > aMCI)						
R precuneus	4,321	9	−61	40	6.31	10^{-4}
L thalamus	154	−14	−16	3	4.27	0.02
R precuneus	45	−17	−45	67	4.24	0.02
L precuneus	24	−2	−39	34	4.42	0.01

GM grey matter, *FDG-PET* glucose consumption, *CS* cluster size (in mm^3). *L* left, *R* right. Coordinates (x–y–z) are in the MNI152 brain anatomical space. *T* values (degrees of freedom in the subscript)

P exact *p* value corresponding to group comparison (FWE corrected, age and gender as covariates)

aMCI group showed decreased levels of neural synchrony ($p < 0.05$, FWE corrected) in 41 of 780 PLIs (5.25 %), no significant results were found in the opposite direction (i.e., aMCI > HO). More than half (51.2 %) of the above significant differences affected functional coupling between left and right hemispheres, whereas 29.2 and 19.5 % of significant differences were restricted to the left and right hemispheres, respectively (Fig. 1, left column). Significant group differences in neural-phase coupling mainly affected relationships between right parietal and left temporo-parietal regions, as well as functional connectivity within the right parietal lobe and between right parietal and right temporal regions. Therefore, the parietal lobe, mainly from the right hemisphere, was the cortical region that accounted for most of the resting-state connectivity failures showed by aMCI subjects.

aMCI ApoE4 carriers also presented a significant reduction of neural-phase coupling in 16 of 780 PLIs (2 %) compared to aMCI ApoE4 non-carriers. As illustrated in Fig. 1 (right column), reduced connectivity in aMCI ApoE4 carriers mainly affected communication between regions of the frontal lobe, and regions of the right frontal and parieto-occipital cortex.

Group differences in GM and glucose consumption of cerebral sources of EEG-alpha rhythm

Table 3 summarizes group differences in GM and glucose consumption (FDG-PET) of cerebral sources involved in the generation of the alpha rhythm ($p < 0.05$, FWE corrected). Figure 2 displays these changes (top panel: GM; bottom panel: FDG-PET) on a volume rendering of cerebral MRI. Briefly, aMCI subjects showed volume reductions of the thalamus, those in the right hemisphere being more accentuated. We further found significant hypometabolism in bilateral regions of the precuneus, and the left
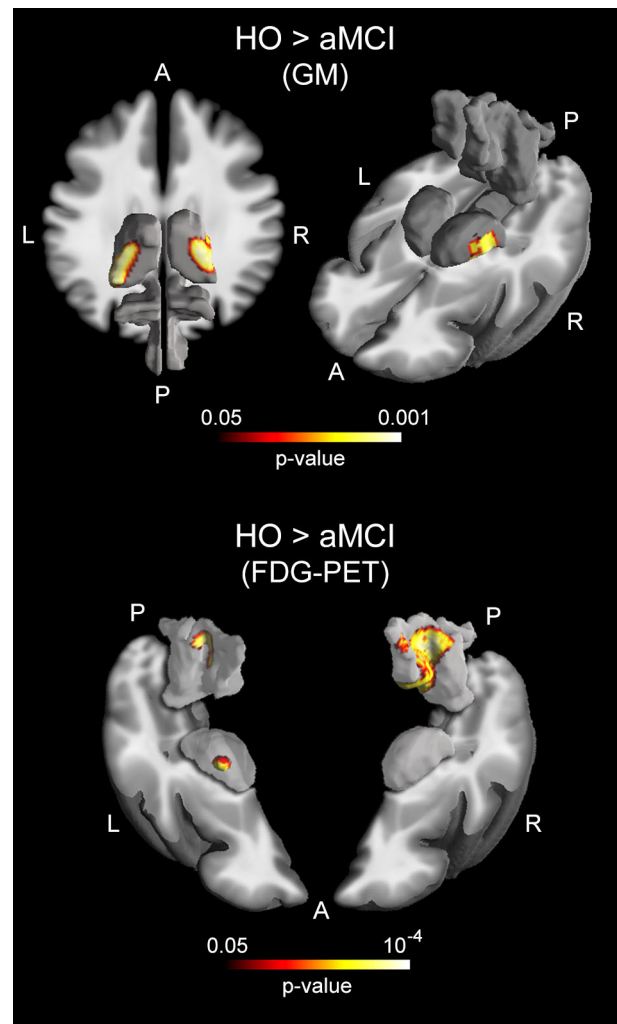

Fig. 2 Group differences in GM and glucose consumption of cerebral regions involved in the generation of alpha rhythms ($p < 0.05$; controlled for FWE). *Upper panel*: GM changes restricted to bilateral regions of the thalamus. *Bottom panel*: FDG-PET changes restricted to bilateral regions of the precuneus and left thalamus. *A* anterior, *P* posterior, *L* left; *R* right

thalamus. No significant differences in GM or glucose consumption were found when comparing aMCI ApoE4 carriers with non-carriers.

Relationship between changes in GM/glucose consumption of EEG-alpha sources and neural-phase coupling

We further investigated whether changes in resting-state alpha connectivity patterns were related to variations in GM/glucose consumption of EEG-alpha sources in HO and aMCI subjects, separately. These analyses revealed positive correlations between GM of the right thalamus and inter-hemispheric coupling of fronto-occipital regions restricted only in HO subjects ($p < 0.02$). Between-group

Table 4 Group differences in correlations between GM and FDG-PET changes in EEG-alpha sources and levels of alpha-phase coupling

Electrode pair	EEG-alpha generator	CS	x	y	z	r	P
GM							
lF–rO HO$^+$ > aMCI$^-$	R thalamus	18	26	−16	9	0.29	0.04
FDG-PET							
rP–rP HO$^+$ > aMCI$^-$	R precuneus	873	−5	−67	42	0.43	0.004
lT–rP HO$^+$ > aMCI$^-$	R precuneus	622	6	−49	25	0.39	0.01
rP–rP HO$^+$ > aMCI$^-$	R precuneus	208	0	−61	36	0.37	0.02

GM grey matter, *FDG-PET* glucose consumption, *CS* cluster size (in mm^3). *l/L* left, *r/R* right. *F* frontal, *P* parietal, *T* temporal, *O* occipital. Coordinates (x–y–z) are in the MNI152 brain space

$^{+/-}$ Denotes the direction of correlations within each group, although only correlations for HO subjects reached significance. *r* Pearson correlation coefficient

P exact *p* value corresponding to between-group regression analyses (FWE-corrected, age and gender as covariates)
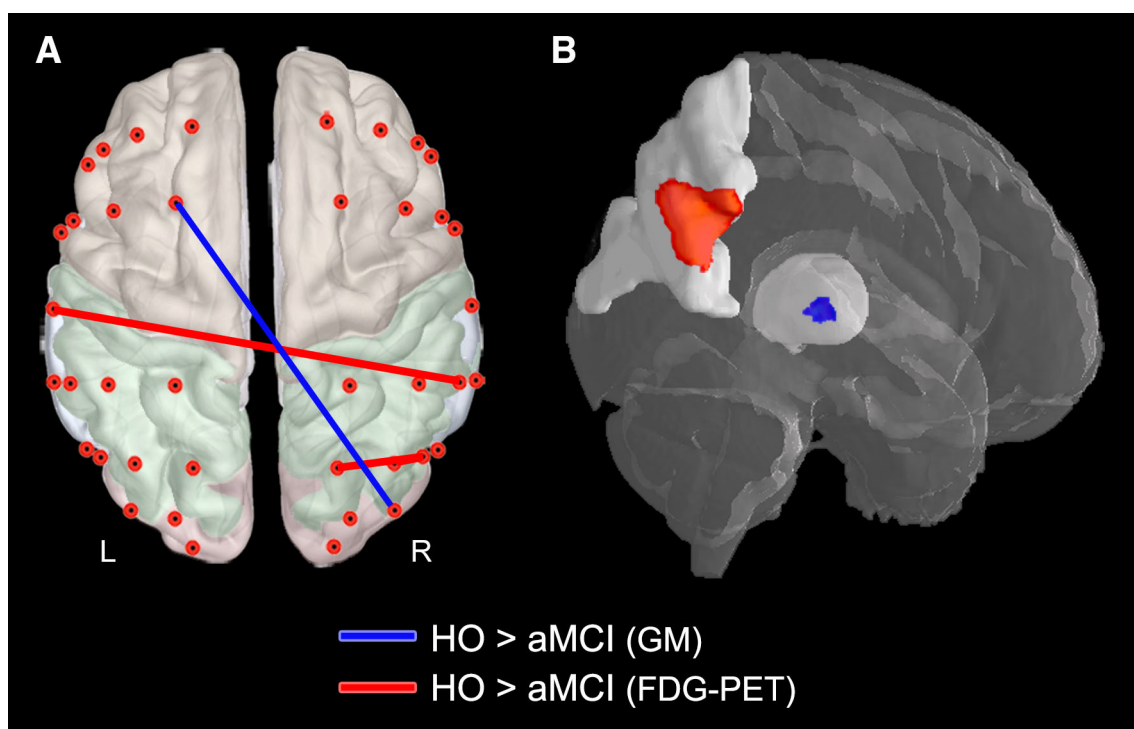

Fig. 3 Relationship between GM/glucose consumption of EEG-alpha cerebral sources and patterns of alpha-phase coupling ($p < 0.05$; controlled for FWE). **a** Cortico-cortical oscillatory coupling involved in significant correlations with GM and FDG-PET changes. **b** Anatomical location of significant correlations. Correlations with GM are represented in *blue*, whereas correlations with FDG-PET are displayed in *red*. *L* left hemisphere, *R* right hemisphere

regression slopes also differed significantly ($p < 0.04$). Additionally, we found positive correlations between glucose consumption of right parietal lobe and alpha coupling of right parietal regions in HO subjects ($0.02 < p < 0.03$). Analysis yielded significant differences when compared regression slopes of the two groups ($0.004 < p < 0.02$). Further information on group differences in regression slopes for correlations between neuroimaging changes and neuroelectric cortical coupling are shown in Table 4 and illustrated in Fig. 3.

No significant relationship between GM/glucose consumption and cortical alpha-phase coupling was found either in aMCI ApoE4 carriers or in non-carriers.

Relationship between changes in Aβ-lipid levels and alpha-phase coupling

We examined whether changes in cortical connectivity patterns underlying alpha rhythms were associated with peripheral Aβ-lipid levels in each group, separately.
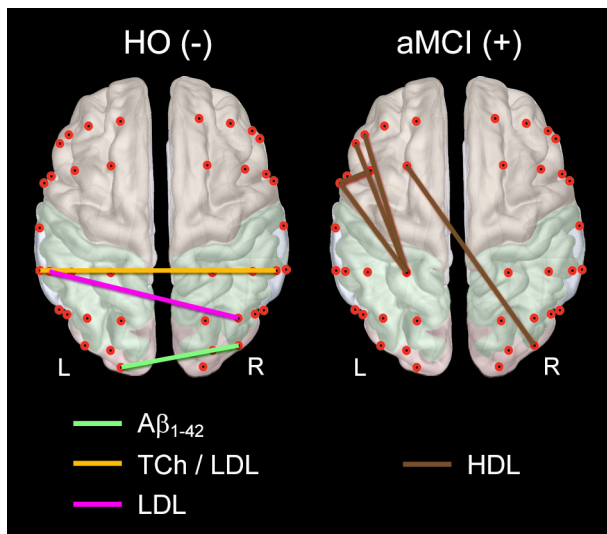
Fig. 4 Relationship between Aβ-lipid levels and alpha-phase coupling in HO (*left panel*) and aMCI subjects (*right panel*). Each significant biological marker was displayed in different color. *Plus/minus* denotes the direction of significant correlations in each group. *Aβ$_{1-42}$* amyloid-beta isoform 42, *TCh* total cholesterol, *LDL* low-density lipoprotein, *HDL* high-density lipoprotein. *L* left, *R* right

Results showed that decreased levels of Aβ$_{1-42}$ ($r = -0.64$, $p < 0.001$), TCh ($r = -0.54$, $p < 0.005$) and LDL ($r = -0.57$, $p < 0.003$; $r = -0.47$, $p < 0.01$) accompanied enhanced inter-hemispheric functional connectivity in HO subjects, although group differences in regression slopes did not reach significance between the two groups. In aMCI subjects, significant correlations were restricted to positive correlations between HDL levels and alpha-phase coupling (r values ranged from 0.41 to 0.47, p values ranged from 0.02 to 0.01) mostly involving the left hemisphere. Comparison of regression slopes revealed significant higher correlations in aMCI than in HO subjects ($p < 0.01$). Figure 4 illustrates significant relationships between Aβ-serum lipid levels and resting-state alpha connectivity patterns in HO (all negative correlations) and aMCI subjects (all positive correlations).

No significant relationship between Aβ-lipid levels and alpha connectivity patterns were found either in aMCI ApoE4 carriers or in non-carriers.

Relationship between Aβ-lipid levels and GM/glucose consumption of EEG-alpha cerebral sources

Finally, we assessed whether Aβ and lipid levels were related to structural/functional changes in cerebral regions involved in the generation of the alpha rhythm. Regression analyses revealed a significant relationship between increased levels of triglycerides and decreased GM of precuneus only in aMCI (r values ranged from 0.5 to 0.57, p values ranged from 0.01 to 0.001). The analysis also yielded significant differences between the regression slopes of the two groups (Table 5; Fig. 5). No significant relationship was found between peripheral blood markers (Aβ or lipids) and glucose consumption either in HO or aMCI subjects. Neither did we find significant associations between Aβ-lipid levels and neuroimaging changes in either aMCI ApoE4 carriers or in non-carriers.

Discussion

In the present study, we have investigated whether changes in EEG-connectivity patterns underlying resting-state are accompanied by macroscopic changes (GM and glucose consumption) in cerebral sources of the alpha rhythm, as well as by changes in peripheral Aβ and lipid levels in HO and aMCI subjects. Results revealed that individuals with aMCI showed hypometabolism in the precuneus, GM atrophy in the thalamus, and enhanced levels of Aβ and ApoB. Contrary to the expected, most of these markers were significantly associated with the strength of neural-phase coupling observed in HO subjects, but not with impaired cortical synchronization proper of aMCI subjects, suggesting that synaptic destabilization associated with incipient neurodegeneration might lead to aberrant structural–functional relationships of alpha EEG sources.

Table 5 Group differences in correlations between triglycerides levels and FDG-PET changes in EEG-alpha sources

	EEG-alpha source	CS	x	y	z	r	P
FDG-PET							
HO$^+$ > aMCI$^-$	R precuneus	669	14	−75	49	0.6	2×10^{-5}
HO$^+$ > aMCI$^-$	L precuneus	332	−9	−76	54	0.5	0.002
HO$^+$ > aMCI$^-$	L precuneus	90	−17	−40	63	0.43	0.01

FDG-PET glucose consumption, *CS* cluster size (in mm^3), *L* left, *R* right. Coordinates (x–y–z) are in the MNI152 brain anatomical space

$^{+/-}$ Denotes the direction of correlations within each group, although only correlations for HO subjects reached significance. *r* Pearson correlation coefficient

P exact *p* value corresponding to between-group regression analyses (FWE-corrected, age and gender as covariates)
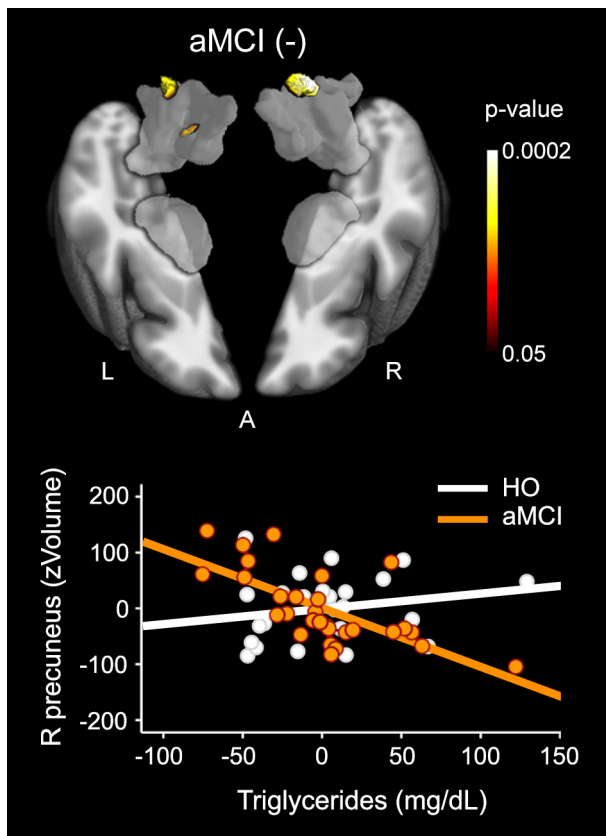
Fig. 5 Relationship between increased levels of triglycerides and decreased GM of precuneus in aMCI subjects ($p < 0.05$; controlled for FWE). *Plus/minus* denotes the direction of significant correlations in each group. *Upper panel*: anatomical location of significant correlations, restricted to bilateral regions of the precuneus. *Bottom panel*: *scatter plot* displaying relationships between GM loss of the right precuneus (*Z*-scored volume of the voxel reached maximum significance) and increased levels of triglycerides. Note that this relationship only reached significance in the aMCI group. *A* anterior, *L* left, *R* right

Interestingly, aMCI subjects showed a positive relationship between levels of HDL cholesterol and the strength of neural-phase coupling, leading to the hypothesis that high concentrations of HDL might have enhanced neuroprotector effects in aMCI. Together, these results provide the first evidence of cerebral and biological correlates of changes in neural oscillatory coupling in two different trajectories of aging.

Failures in resting-state cerebral networks reveal the unbalance between structure and function in aMCI

Synapse dysfunction, the major neurobiological correlate of cognitive impairment in AD (DeKosky and Scheff 1990; Terry et al. 1991), has shown to precede tangle formation and neuronal loss in MCI subjects (Masliah et al. 2001; Scheff et al. 2006). Most of the synaptic degeneration in

neocortex affects large pyramidal neurons of layers III and V, largely connected through cortico-cortical association fibers (Terry et al. 1981; Rogers and Morrison 1985; Hof et al. 1990). Consequently, and given that oscillatory EEG activity results from summated excitatory and inhibitory postsynaptic potentials primarily generated by synaptic activity of large pyramidal neurons in the cerebral cortex (Lopes da Silva and Van Rotterdam 1993), synaptic dysfunction occurring in aMCI subjects may be reflected in abnormal patterns of EEG coupling. Accordingly, resting-state EEG alpha rhythms not only are significantly different in aMCI when compared with HO subjects (Babiloni et al. 2006a; Cantero et al. 2009a), but they are also able to predict progressive cognitive deterioration (Babiloni et al. 2014) and stability of MCI status over time (Babiloni et al. 2011). However, up to now only a few studies have established a link between abnormalities of EEG rhythms and cortical atrophy in aMCI subjects (Babiloni et al. 2006b, 2013). The present study gives a step further in evaluating the link between failures in resting-state large-scale synchronization mechanisms and the anatomo-functional integrity of cerebral sources involved in the generation of alpha rhythms.

We showed structural and functional changes of the thalamus and precuneus in aMCI subjects, two regions considered canonical neuroelectric sources of EEG alpha rhythms (Cantero et al. 2009a, b). Accumulated evidence supports a complex relationship between the thalamus and neocortex during generation of alpha oscillations. For instance, increased glucose consumption of the thalamus is paralleled by increased amplitude of alpha oscillations over parieto-occipital regions (Goldman et al. 2002; Schreckenberger et al. 2004; Feige et al. 2005; De Munck et al. 2007). Furthermore, cortical and thalamic regions are highly coherent during generation of alpha waves (Lopes da Silva et al. 1973). Therefore, bilateral GM loss of thalamus characterizing our aMCI sample might account for impaired alpha connectivity between anterior and posterior regions of the brain, likely due to synaptic dysfunction or synaptic loss of thalamocortical neurons. This hypothesis is supported by studies showing amyloid deposits and neurofibrillary tangles in the thalamus of AD patients (Rudelli et al. 1984; Masliah et al. 1989; Braak and Braak 1991) together with significant GM loss (Karas et al. 2004) that further correlated with impaired cognitive functioning (de Jong et al. 2008), and by studies showing altered patterns of functional connectivity between thalamus and precuneus in aMCI subjects (Cantero et al. 2009a; Wang et al. 2012; Zhou et al. 2013).

The precuneus is a region of the superior parietal lobe also involved in EEG-alpha generation (Toth et al. 2007; Michels et al. 2008; Cantero et al. 2009a). An emerging

body of evidence suggests that this area is extremely vulnerable to the accumulation of Aβ plaques during the progression of AD (Rowe et al. 2007; Driscoll et al. 2012), which might account for disrupted connectivity with other brain regions in amyloid-positive MCI subjects (Drzezga et al. 2011), as well as for cognitive decline in preclinical AD patients (Nickl-Jockschat et al. 2012; Yotter et al. 2013).

Contrary to our initial hypothesis, neither GM loss in the thalamus nor hypometabolism in the precuneus were correlated with the strength of alpha phase synchrony in aMCI subjects. This relationship only emerged in HO adults. Aging-related changes in synaptic loss likely accounted for coherent relationships between structure and function in normal aging, whereas synaptic dysfunctions in aMCI might lead to the lack of significant associations between damage of cerebral sources of alpha rhythm and failures in EEG alpha coupling.

Relationship between peripheral blood markers and patterns of resting-state cortical connectivity in HO and aMCI

Searching for reliable peripheral blood markers of incipient neurodegeneration is increasingly important, given the invasive nature, potential side effects, and problematic follow-up analysis based on CSF sample collections. However, results derived from cross-sectional studies using plasma Aβ in MCI patients are largely inconsistent (Sobów et al. 2005; Blasko et al. 2008; Storace et al. 2010; Pesini et al. 2012), likely due to the instability of Aβ peptides in plasma (Humpel 2011), the state of aggregation (Storace et al. 2010), and the heterogeneity of MCI populations across studies. In agreement with our results, only those studies that specifically included MCI of an amnestic type have found higher plasma levels of $Aβ_{1–42}$ compared to HO subjects (Storace et al. 2010; Sobów et al. 2005; Pesini et al. 2012). Although increased levels of plasma $Aβ_{1–42}$ observed in aMCI subjects might be signalling a central pathogenic process of AD, e.g., deregulation of β-APP metabolism followed by brain Aβ accumulation, this hypothesis still requires experimental confirmation.

Interestingly, we found that elevated levels of $Aβ_{1–42}$ correlated with decreased parieto-occipital functional connectivity in HO, but not in aMCI subjects. This result suggests that plasma levels of $Aβ_{1–42}$ is a better marker of normal aging-related changes in alpha cortical networks than of aMCI-related changes, and, in turn, might be tentatively proposed as a surrogate marker of aging-related decline in cortical function. An alternative explanation for this result is that cognitively normal elderly with elevated concentrations of $Aβ_{1–42}$ might present a faster cognitive decline rate over time. This hypothesis is supported by

studies showing that an increased Aβ plaque burden, assessed with [(11)C]Pittsburgh compound B (PiB), is significantly associated with worsening of different cognitive domains (Wirth et al. 2013) and with cortical thinning in clinically normal elderly (Becker et al. 2011). Recent studies have also found significant associations between subjective cognitive complaints and PiB uptake in HO adults (Amariglio et al. 2012), mostly affecting medial prefrontal cortex, cingulate cortex, and precuneus (Perrotin et al. 2012). Subjective cognitive complaints might be related to increased plasma levels of $Aβ_{1–42}$ in HO subjects, accounting for failures in parieto-occipital functional connectivity observed in our study. Given that the presence of subjective cognitive complaints was not specifically assessed in HO subjects of our study, further investigation needs to be performed to clarify this hypothesis. Furthermore, the sample used in this study was relatively small and lacked in vivo markers of AD pathology (i.e., CSF Aβ-tau and/or amyloid-PET), impeding confirmation of preclinical AD in our aMCI sample. Therefore, further longitudinal research combining plasma Aβ and other biomarkers in non-demented older adults and preclinical AD, confirmed by CSF Aβ and/or amyloid-PET markers, is clearly needed to determine whether plasma Aβ has diagnostic value in combination with other biomarkers.

Lipid markers correlate with resting-state cortical connectivity patterns in HO and aMCI

Considerable evidence supports a pathogenic link between the deregulation of cholesterol homeostasis and AD (Roher et al. 1999; Wood et al. 1999). Early findings have shown that elevated cholesterol levels are an early risk factor for developing AD (Pappolla et al. 2003), sustaining the hypothesis that cholesterol plays a role in promoting amyloidogenesis (Bodovitz and Klein 1996; Simons et al. 1998; Refolo et al. 2000; Grösgen et al. 2010). However, our study is the first in assessing associations between serum lipid levels and oscillatory cortical connectivity in HO and aMCI subjects, and in establishing a link between these markers and macroscopic changes in cerebral regions involved in the generation of the human resting-state alpha rhythm.

We have shown that ApoB levels, the best estimate of circulating lipoproteins with atherogenic potential (Barter et al. 2006), were significantly elevated in aMCI subjects, confirming early findings reported in AD patients (Caramelli et al. 1999). Evidence has shown that high ApoB (Motta et al. 2009) and high LDL cholesterol levels (Lamarche et al. 1996) predict atherogenic alterations. Accordingly, cardiovascular risk factors have been found as predictive markers of faster conversion to AD through different pathophysiological mechanisms derived from

vascular pathology (Tabet et al. 2009; Peters and Beckett 2009). Although triglyceride levels did not differ in our study, their increase was associated with bilateral GM loss in precuneus of aMCI subjects. Evidence has shown significant associations between triglycerides and elevated peripheral Aβ levels in murine AD models (Burgess et al. 2006), although molecular mechanisms underlying this relationship remain to be fully defined.

Promoting successful cognitive aging is a topic of major importance to the field of public health. Different patterns of cognitive aging have been identified in the last two decades, and there is growing need to better understand what influences these trajectories. For instance, factors that impact cholesterol metabolism, such as dietary intake or physical activity, play an important role in late-life cognitive function and the risk of dementia. In our study, the strength of oscillatory cortical connectivity patterns (mostly in the left hemisphere) of aMCI subjects benefitted from increased levels of HDL, whereas inter-hemispheric connectivity loss in HO was associated with increased levels of total and LDL cholesterol. These results reveal, for the first time, that serum lipid levels in normal and pathological aging relate differently to resting-state functional networks and to macroscopic changes in cerebral sources of alpha rhythms. The relationship between altered lipid metabolism and cognitive function in aging and AD is likely indirect, due to the lack of positive effects of statins on cognitive performance in normal aging (Benito-Leon et al. 2010; Richardson et al. 2013) or their inability to prevent AD (Ancelin et al. 2012; Swiger et al. 2013). In summary, our findings provide a novel framework for establishing cerebral correlates of lipid levels in healthy aging and in older adults with aMCI. Major effort aimed at identifying modifiable cardiovascular risk factors will definitively promote successful cognitive aging and will lead to novel strategies to prevent dementia in the near future.

References

Amariglio RE, Becker JA, Carmasin J, Wadsworth LP, Lorius N, Sullivan C, Maye JE, Gidicsin C, Pepin LC, Sperling RA, Johnson KA, Rentz DM (2012) Subjective cognitive complaints and amyloid burden in cognitively normal older individuals. Neuropsychologia 50:2880–2886

Ancelin ML, Carrière I, Barberger-Gateau P, Auriacombe S, Rouaud O, Fourlanos S, Berr C, Dupuy AM, Ritchie K (2012) Lipid lowering agents, cognitive decline, and dementia: the three-city study. J Alzheimers Dis 30:629–637

Arnold SE, Hyman BT, Flory J, Damasio AR, Van Hoesen GW (1991) The topographical and neuroanatomical distribution of neurofibrillary tangles and neuritic plaques in the cerebral cortex of patients with Alzheimer's disease. Cereb Cortex 1:103–116

Ashburner J (2007) A fast diffeomorphic image registration algorithm. Neuroimage 38:95–113

Ashburner J, Friston KJ (2000) Voxel-based morphometry—the methods. Neuroimage 11:805–821

Babiloni C, Ferri R, Moretti DV, Strambi A, Binetti G, Dal Forno G, Ferreri F, Lanuzza B, Bonato C, Nobili F, Rodriguez G, Salinari S, Passero S, Rocchi R, Stam CJ, Rossini PM (2004) Abnormal fronto-parietal coupling of brain rhythms in mild Alzheimer's disease: a multicentric EEG study. Eur J Neurosci 19:2583–2590

Babiloni C, Ferri R, Binetti G, Cassarino A, Dal Forno G, Ercolani M, Ferreri F, Frisoni GB, Lanuzza B, Miniussi C, Nobili F, Rodriguez G, Rundo F, Stam CJ, Musha T, Vecchio F, Rossini PM (2006a) Fronto-parietal coupling of brain rhythms in mild cognitive impairment: a multicentric EEG study. Brain Res Bull 69:63–73

Babiloni C, Frisoni G, Steriade M, Bresciani L, Binetti G, Del Percio C, Geroldi C, Miniussi C, Nobili F, Rodriguez G, Zappasodi F, Carfagna T, Rossini PM (2006b) Frontal white matter volume and delta EEG sources negatively correlate in awake subjects with mild cognitive impairment and Alzheimer's disease. Clin Neurophysiol 117:1113–1129

Babiloni C, Frisoni GB, Vecchio F, Lizio R, Pievani M, Cristina G, Fracassi C, Vernieri F, Rodriguez G, Nobili F, Ferri R, Rossini PM (2011) Stability of clinical condition in mild cognitive impairment is related to cortical sources of alpha rhythms: an electroencephalographic study. Hum Brain Mapp 32:1916–1931

Babiloni C, Carducci F, Lizio R, Vecchio F, Baglieri A, Bernardini S, Cavedo E, Bozzao A, Buttinelli C, Esposito F, Giubilei F, Guizzaro A, Marino S, Montella P, Quattrocchi CC, Redolfi A, Soricelli A, Tedeschi G, Ferri R, Rossi-Fedele G, Ursini F, Scrascia F, Vernieri F, Pedersen TJ, Hardemark HG, Rossini PM, Frisoni GB (2013) Resting state cortical electroencephalographic rhythms are related to gray matter volume in subjects with mild cognitive impairment and Alzheimer's disease. Hum Brain Mapp 34:1427–1446

Babiloni C, Del Percio C, Lizio R, Marzano N, Infarinato F, Soricelli A, Salvatore E, Ferri R, Bonforte C, Tedeschi G, Montella P, Baglieri A, Rodriguez G, Famà F, Nobili F, Vernieri F, Ursini F, Mundi C, Frisoni GB, Rossini PM (2014) Cortical sources of resting state electroencephalographic alpha rhythms deteriorate across time in subjects with amnesic mild cognitive impairment. Neurobiol Aging 35:130–142

Barter PJ et al (2006) Apo B versus cholesterol in estimating cardiovascular risk and in guiding therapy: report of the thirty-person/ten-country panel. J Intern Med 259:247–258

Becker JA, Hedden T, Carmasin J, Maye J, Rentz DM, Putcha D, Fischl B, Greve DN, Marshall GA, Salloway S, Marks D, Buckner RL, Sperling RA, Johnson KA (2011) Amyloid-β associated cortical thinning in clinically normal elderly. Ann Neurol 69:1032–1042

Benito-Leon J, Louis ED, Vega S, Bermejo-Pareja F (2010) Statins and cognitive functioning in the elderly: a population-based study. J Alzheimers Dis 21:95–102

Bishop NA, Lu T, Yankner BA (2010) Neural mechanisms of ageing and cognitive decline. Nature 464:529–535

Blasko I, Jellinger K, Kemmler G, Krampla W, Jungwirth S, Wichart I, Tragl KH, Fischer P (2008) Conversion from cognitive health to mild cognitive impairment and Alzheimer's disease: prediction by plasma amyloid beta 42, medial temporal lobe atrophy and homocysteine. Neurobiol Aging 29:1–11

Blesa R, Pujol M, Aguilar M, Santacruz P, Bertran-Serra I, Hernández G, Sol JM, Peña-Casanova J, NORMACODEM Group (2001) Clinical validity of the 'mini-mental state' for Spanish speaking communities. Neuropsychologia 39:1150–1157

Bodovitz S, Klein WL (1996) Cholesterol modulates alpha-secretase cleavage of amyloid precursor protein. J Biol Chem 271:4436–4440

Braak H, Braak E (1991) Demonstration of amyloid deposits and neurofibrillary changes in whole brain sections. Brain Pathol 1:213–216

Brier MR, Thomas JB, Snyder AZ, Benzinger TL, Zhang D, Raichle ME, Holtzman DM, Morris JC, Ances BM (2012) Loss of intranetwork and internetwork resting state functional connections with Alzheimer's disease progression. J Neurosci 32:8890–8899

Burgess BL, McIsaac SA, Naus KE, Chan JY, Tansley GH, Yang J, Miao F, Ross CJ, van Eck M, Hayden MR, van Nostrand W, St George-Hyslop P, Westaway D, Wellington CL (2006) Elevated plasma triglyceride levels precede amyloid deposition in Alzheimer's disease mouse models with abundant A beta in plasma. Neurobiol Dis 24:114–127

Cantero JL, Atienza M, Gomez-Herrero G, Cruz-Vadell A, Gil-Neciga E, Rodriguez-Romero R, Garcia-Solis D (2009a) Functional integrity of thalamocortical circuits differentiates normal aging from mild cognitive impairment. Hum Brain Mapp 30:3944–3957

Cantero JL, Atienza M, Cruz-Vadell A, Suarez-Gonzalez A, Gil-Neciga E (2009b) Increased synchronization and decreased neural complexity underlie thalamocortical oscillatory dynamics in mild cognitive impairment. Neuroimage 46:938–948

Cao L, Schrank BR, Rodriguez S, Benz EG, Moulia TW, Rickenbacher GT, Gomez AC, Levites Y, Edwards SR, Golde TE, Hyman BT, Barnea G, Albers MW (2012) Aβ alters the connectivity of olfactory neurons in the absence of amyloid plaques in vivo. Nat Commun 3:1009

Caramelli P, Nitrini R, Maranhão R, Lourenço AC, Damasceno MC, Vinagre C, Caramelli B (1999) Increased apolipoprotein B serum concentration in Alzheimer's disease. Acta Neurol Scand 100:61–63

Cheng N, Bai L, Steuer E, Belluscio L (2013) Olfactory functions scale with circuit restoration in a rapidly reversible Alzheimer's disease model. J Neurosci 33:12208–12217

De Jong LW, Van der Hiele K, Veer IM, Houwing JJ, Westendorp RG, Bollen EL, De Bruin PW, Middelkoop HA, Van Buchem MA, Van der Grond J (2008) Strongly reduced volumes of putamen and thalamus in Alzheimer's disease: an MRI study. Brain 131:3277–3285

De Munck JC, Gonçalves SI, Huijboom L, Kuijer JP, Pouwels PJ, Heethaar RM, Lopes da Silva FH (2007) The hemodynamic response of the alpha rhythm: an EEG/fMRI study. Neuroimage 35:1142–1151

DeKosky ST, Scheff SW (1990) Synapse loss in frontal cortex biopsies in Alzheimer's disease: correlation with cognitive severity. Ann Neurol 27:457–464

Di Paolo G, Kim TW (2011) Linking lipids to Alzheimer's disease: cholesterol and beyond. Nat Rev Neurosci 12:284–296

Driscoll I, Troncoso JC, Rudow G, Sojkova J, Pletnikova O, Zhou Y, Kraut MA, Ferrucci L, Mathis CA, Klunk WE, O'Brien RJ, Davatzikos C, Wong DF, Resnick SM (2012) Correspondence between in vivo (11)C-PiB-PET amyloid imaging and post-mortem, region-matched assessment of plaques. Acta Neuropathol 124:823–831

Drzezga A, Becker JA, Van Dijk KR, Sreenivasan A, Talukdar T, Sullivan C, Schultz AP, Sepulcre J, Putcha D, Greve D, Johnson KA, Sperling RA (2011) Neuronal dysfunction and disconnection of cortical hubs in non-demented subjects with elevated amyloid burden. Brain 134:1635–1646

Fazekas F, Chawluk JB, Alavi A, Hurtig HI, Zimmerman RA (1987) MR signal abnormalities at 1.5 T in Alzheimer's dementia and normal aging. Am J Roentgenol 149:351–356

Feige B, Scheffler K, Esposito F, Di Salle F, Hennig J, Seifritz E (2005) Cortical and subcortical correlates of electroencephalographic alpha rhythm modulation. J Neurophysiol 93:2864–2872

Fischl B, Sereno MI, Dale AM (1999a) Cortical surface-based analysis. II: inflation, flattening, and a surface-based coordinate system. Neuroimage 9:195–207

Fischl B, Sereno MI, Tootell RB, Dale AM (1999b) High-resolution intersubject averaging and a coordinate system for the cortical surface. Hum Brain Mapp 8:272–284

Ghribi O (2008) Potential mechanisms linking cholesterol to Alzheimer's disease-like pathology in rabbit brain, hippocampal organotypic slices, and skeletal muscle. J Alzheimers Dis 15:673–684

Giovacchini G, Lerner A, Toczek MT, Fraser C, Ma K, DeMar JC, Herscovitch P, Eckelman WC, Rapoport SI, Carson RE (2004) Brain incorporation of 11C-arachidonic acid, blood volume, and blood flow in healthy aging: a study with partial-volume correction. J Nucl Med 45:1471–1479

Goldman RI, Stern JM, Engel J Jr, Cohen MS (2002) Simultaneous EEG and fMRI of the alpha rhythm. Neuroreport 13:2487–2492

Graff-Radford NR, Crook JE, Lucas J, Boeve BF, Knopman DS, Ivnik RJ, Smith GE, Younkin LH, Petersen RC, Younkin SG (2007) Association of low plasma Abeta42/Abeta40 ratios with increased imminent risk for mild cognitive impairment and Alzheimer disease. Arch Neurol 64:354–362

Greicius MD, Srivastava G, Reiss AL, Menon V (2004) Default-mode network activity distinguishes Alzheimer's disease from healthy aging: evidence from functional MRI. Proc Natl Acad Sci USA 101:4637–4642

Grimm MO, Grimm HS, Tomic I, Beyreuther K, Hartmann T, Bergmann C (2008) Independent inhibition of Alzheimer disease beta- and gamma-secretase cleavage by lowered cholesterol levels. J Biol Chem 283:11302–11311

Grösgen S, Grimm MO, Friess P, Hartmann T (2010) Role of amyloid beta in lipid homeostasis. Biochim Biophys Acta 1801:966–974

Hof PR, Morrison JH (2004) The aging brain: morphomolecular senescence of cortical circuits. Trends Neurosci 27:607–613

Hof PR, Cox K, Morrison JH (1990) Quantitative analysis of a vulnerable subset of pyramidal neurons in Alzheimer's disease: I. SUPERIOR frontal and inferior temporal cortex. J Comp Neurol 301:44–54

Hsia AY, Masliah E, McConlogue L, Yu GQ, Tatsuno G, Hu K, Kholodenko D, Malenka RC, Nicoll RA, Mucke L (1999) Plaque-independent disruption of neural circuits in Alzheimer's disease mouse models. Proc Natl Acad Sci USA 96:3228–32233

Hughes SW, Lörincz M, Cope DW, Blethyn KL, Kekesi KA, Parri HR, Juhasz G, Crunelli V (2004) Synchronized oscillations at alpha and theta frequencies in the lateral geniculate nucleus. Neuron 42:253–268

Humpel C (2011) Identifying and validating biomarkers for Alzheimer's disease. Trends Biotechnol 29:26–32

Iacono D, Markesbery WR, Gross M, Pletnikova O, Rudow G, Zandi P, Troncoso JC (2009) The Nun study: clinically silent AD, neuronal hypertrophy, and linguistic skills in early life. Neurology 73:665–673

Karas GB, Scheltens P, Rombouts SA, Visser PJ, van Schijndel RA, Fox NC, Barkhof F (2004) Global and local gray matter loss in mild cognitive impairment and Alzheimer's disease. Neuroimage 23:708–716

Katzman R, Terry R, DeTeresa R, Brown T, Davies P, Fuld P, Renbing X, Peck A (1988) Clinical, pathological, and neurochemical changes in dementia: a subgroup with preserved mental status and numerous neocortical plaques. Ann Neurol 23:138–144

Koyama A, Okereke OI, Yang T, Blacker D, Selkoe DJ, Grodstein F (2012) Plasma amyloid-β as a predictor of dementia and cognitive decline: a systematic review and meta-analysis. Arch Neurol 69:824–831

Lachaux JP, Rodriguez E, Martinerie J, Varela FJ (1999) Measuring phase synchrony in brain signals. Hum Brain Mapp 8:194–208

Lacor PN, Buniel MC, Furlow PW, Clemente AS, Velasco PT, Wood M, Viola KL, Klein WL (2007) Aβ oligomer-induced aberrations in synapse composition, shape, and density provide a molecular basis for loss of connectivity in Alzheimer's disease. J Neurosci 27:796–807

Lamarche B, Moorjani S, Lupien PJ, Cantin B, Bernard PM, Dagenais GR, Després JP (1996) Apolipoprotein A-I and B levels and the risk of ischemic heart disease during a five-year follow-up of men in the Québec cardiovascular study. Circulation 94:273–278

Lambert MP, Barlow AK, Chromy BA, Edwards C, Freed R, Liosatos M, Morgan TE, Rozovsky I, Trommer B, Viola KL, Wals P, Zhang C, Finch CE, Krafft GA, Klein WL (1998) Diffusible, nonfibrillar ligands derived from Abeta1–42 are potent central nervous system neurotoxins. Proc Natl Acad Sci USA 95:6448–6453

Leritz EC, Salat DH, Williams VJ, Schnyer DM, Rudolph JL, Lipsitz L, Fischl B, McGlinchey RE, Milberg WP (2011) Thickness of the human cerebral cortex is associated with metrics of cerebrovascular health in a normative sample of community dwelling older adults. Neuroimage 54:2659–26571

Lesné S, Koh MT, Kotilinek L, Kayed R, Glabe CG, Yang A, Gallagher M, Ashe KH (2006) A specific amyloid-beta protein assembly in the brain impairs memory. Nature 440:352–357

Lopes da Silva F (1991) Neural mechanisms underlying brain waves: from neural membranes to networks. Electroencephalogr Clin Neurophysiol 79:81–93

Lopes da Silva F, Van Rotterdam A (1993) Biophysical aspects of EEG and magnetoencephalogram generation. In: Niedermeyer E, Lopes da Silva FH (eds) Electroencephalography. Basic principles, clinical applications and related fields. Williams and Wilkins, Baltimore, pp 78–91

Lopes da Silva FH, van Lierop TH, Schrijer CF, van Leeuwen WS (1973) Organization of thalamic and cortical alpha rhythms: spectra and coherences. Electroencephalogr Clin Neurophysiol 35:627–639

Maris E (2004) Randomization tests for ERP topographies and whole spatiotemporal data matrices. Psychophysiology 41:142–151

Martins IJ, Berger T, Sharman MJ, Verdile G, Fuller SJ, Martins RN (2009) Cholesterol metabolism and transport in the pathogenesis of Alzheimer's disease. J Neurochem 111:1275–1308

Masliah E, Terry R, Buzsaki G (1989) Thalamic nuclei in Alzheimer disease: evidence against the cholinergic hypothesis of plaque formation. Brain Res 493:241–246

Masliah E, Mallory M, Hansen L, DeTeresa R, Terry RD (1993) Quantitative synaptic alterations in the human neocortex during normal aging. Neurology 43:192–197

Masliah E, Mallory M, Alford M, DeTeresa R, Hansen LA, McKeel DW Jr, Morris JC (2001) Altered expression of synaptic proteins occurs early during progression of Alzheimer's disease. Neurology 56:127–129

Michels L, Moazami-Goudarzi M, Jeanmonod D, Sarnthein J (2008) EEG alpha distinguishes between cuneal and precuneal activation in working memory. Neuroimage 40:1296–1310

Miller S, Dykes D, Polesky H (1988) A simple salting out procedure for extracting DNA from human nucleated cells. Nucleic Acids Res 16:1215

Motta M, Bennati E, Cardillo E, Ferlito L, Passamonte M, Malaguarnera M (2009) The significance of apolipoprotein-B (Apo-B) in the elderly as a predictive factor of cardio-cerebrovascular complications. Arch Gerontol Geriatr 49:162–164

Mucke L, Masliah E, Yu GQ, Mallory M, Rockenstein EM, Tatsuno G, Hu K, Kholodenko D, Johnson-Wood K, McConlogue L (2000) High-level neuronal expression of abeta 1-42 in wild-type human amyloid protein precursor transgenic mice: synaptotoxicity without plaque formation. J Neurosci 20:4050–4058

Nickl-Jockschat T, Kleiman A, Schulz JB, Schneider F, Laird AR, Fox PT, Eickhoff SB, Reetz K (2012) Neuroanatomic changes and their association with cognitive decline in mild cognitive impairment: a meta-analysis. Brain Struct Funct 217:115–125

Palop JJ, Chin J, Roberson ED, Wang J, Thwin MT, Bien-Ly N, Yoo J, Ho KO, Yu GQ, Kreitzer A, Finkbeiner S, Noebels JL, Mucke L (2007) Aberrant excitatory neuronal activity and compensatory remodeling of inhibitory hippocampal circuits in mouse models of Alzheimer's disease. Neuron 55:697–711

Panza F, D'Introno A, Colacicco AM, Capurso C, Pichichero G, Capurso SA, Capurso A, Solfrizzi V (2006) Lipid metabolism in cognitive decline and dementia. Brain Res Rev 51:275–292

Pappolla MA, Bryant-Thomas TK, Herbert D, Pacheco J, Fabra Garcia M, Manjon M, Girones X, Henry TL, Matsubara E, Zambon D, Wolozin B, Sano M, Cruz-Sanchez FF, Thal LJ, Petanceska SS, Refolo LM (2003) Mild hypercholesterolemia is an early risk factor for the development of Alzheimer amyloid pathology. Neurology 61:199–205

Pereda E, Quian Quiroga R, Bhattacharya J (2005) Nonlinear multivariate analysis of neurophysiological signals. Prog Neurobiol 77:1–37

Perrotin A, Mormino EC, Madison CM, Hayenga AO, Jagust WJ (2012) Subjective cognition and amyloid deposition imaging: a Pittsburgh Compound B positron emission tomography study in normal elderly individuals. Arch Neurol 69:223–229

Pesini P, Pérez-Grijalba V, Monleón I, Boada M, Tárraga L, Martínez-Lage P, San-José I, Sarasa M (2012) Reliable measurements of the β-amyloid pool in blood could help in the early diagnosis of AD. Int J Alzheimers Dis 2012:604141

Peters R, Beckett N (2009) Hypertension, dementia, and antihypertensive treatment: implications for the very elderly. Curr Hypertens Rep 11:277–282

Petersen PR, Smith GE, Waring SC, Ivnik RJ, Tangalos EG, Kokmen E (1999) Mild cognitive impairment. Clinical characterization and outcome. Arch Neurol 56:303–308

Price JL, Morris JC (1999) Tangles and plaques in nondemented aging and "preclinical" Alzheimer's disease. Ann Neurol 45:358–368

Price JL, Davis PB, Morris JC, White DL (1991) The distribution of tangles, plaques and related immunohistochemical markers in healthy aging and Alzheimer's disease. Neurobiol Aging 12:295–312

Refolo LM, Malester B, LaFrancois J, Bryant-Thomas T, Wang R, Tint GS, Sambamurti K, Duff K, Pappolla MA (2000) Hypercholesterolemia accelerates the Alzheimer's amyloid pathology in a transgenic mouse model. Neurobiol Dis 7:321–331

Richardson K, Schoen M, French B, Umscheid CA, Mitchell MD, Arnold SE, Heidenreich PA, Rader DJ, deGoma EM (2013) Statins and cognitive function: a systematic review. Ann Intern Med 159:688–697

Rogers J, Morrison JH (1985) Quantitative morphology and regional and laminar distribution of senile plaques in Alzheimer's disease. J Neurosci 5:2801–2808

Roher AE, Kuo YM, Kokjohn KM, Emmerling MR, Gracon S (1999) Amyloid and lipids in the pathology of Alzheimer disease. Amyloid 6:136–145

Rowe CC, Ng S, Ackermann U, Gong SJ, Pike K, Savage G, Cowie TF, Dickinson KL, Maruff P, Darby D, Smith C, Woodward M, Merory J, Tochon-Danguy H, O'Keefe G, Klunk WE, Mathis CA, Price JC, Masters CL, Villemagne VL (2007) Imaging beta-amyloid burden in aging and dementia. Neurology 68:1718–1725

Rudelli RD, Ambler MW, Wisniewski HM (1984) Morphology and distribution of Alzheimer neuritic (senile) and amyloid plaques in striatum and diencephalon. Acta Neuropathol 64:273–281

Scheff SW, Price DA, Schmitt FA, Mufson EJ (2006) Hippocampal synaptic loss in early Alzheimer's disease and mild cognitive impairment. Neurobiol Aging 27:1372–1384

Schiff SJ (2005) Dangerous phase. Neuroinformatics 3:315–318

Schreckenberger M, Lange-Asschenfeldt C, Lochmann M, Mann K, Siessmeier T, Buchholz HG, Bartenstein P, Gründer G (2004) The thalamus as the generator and modulator of EEG alpha rhythm: a combined PET/EEG study with lorazepam challenge in humans. Neuroimage 22:637–644

Shobab LA, Hsiung GY, Feldman HH (2005) Cholesterol in Alzheimer's disease. Lancet Neurol 4:841–852

Silva LR, Amitai Y, Connors BW (1991) Intrinsic oscillations of neocortex generated by layer 5 pyramidal neurons. Science 251:432–435

Simons M, Keller P, De Strooper B, Beyreuther K, Dotti CG, Simons K (1998) Cholesterol depletion inhibits the generation of beta-amyloid in hippocampal neurons. Proc Natl Acad Sci USA 95:6460–6464

Snowdon DA, Nun Study (2003) Healthy aging and dementia: findings from the Nun Study. Ann Intern Med 139:450–454

Sobów T, Flirski M, Kłoszewska I, Liberski PP (2005) Plasma levels of alpha beta peptides are altered in amnestic mild cognitive impairment but not in sporadic Alzheimer's disease. Acta Neurobiol Exp (Wars) 65:117–124

Stam CJ, Jones BF, Manshanden I, van Cappellen van Walsum AM, Montez T, Verbunt JPA, de Munck JC, van Dijk BW, Berendse HW, Scheltens P (2006) Magnetoencephalographic evaluation of resting-state functional connectivity in Alzheimer's disease. Neuroimage 32:1335–1344

Stam CJ, Nolte G, Daffertshofer A (2007) Phase lag index: assessment of functional connectivity from multi channel EEG and MEG with diminished bias from common sources. Hum Brain Mapp 28:1178–1193

Storace D, Cammarata S, Borghi R, Sanguineti R, Giliberto L, Piccini A, Pollero V, Novello C, Caltagirone C, Smith MA, Bossù P, Perry G, Odetti P, Tabaton M (2010) Elevation of beta-amyloid 1-42 autoantibodies in the blood of amnestic patients with mild cognitive impairment. Arch Neurol 67:867–872

Sun X, Bhadelia R, Liebson E, Bergethon P, Folstein M, Zhu JJ, Mwamburi DM, Patz S, Qiu WQ (2011) The relationship between plasma amyloid-β peptides and the medial temporal lobe in the homebound elderly. Int J Geriatr Psychiatry 26:593–601

Swiger KJ, Manalac RJ, Blumenthal RS, Blaha MJ, Martin SS (2013) Statins and cognition: a systematic review and meta-analysis of short- and long-term cognitive effects. Mayo Clin Proc 88:1213–1221

Tabet N, Quinn R, Klugman A (2009) Prevalence and cognitive impact of cerebrovascular findings in Alzheimer's disease: a retrospective, naturalistic study. Int J Clin Pract 63:338–345

Terry RD, Peck A, DeTeresa R, Schechter R, Horoupian DS (1981) Some morphometric aspects of the brain in senile dementia of the Alzheimer type. Ann Neurol 10:184–192

Terry RD, Masliah E, Salmon DP, Butters N, DeTeresa R, Hill R, Hansen LA, Katzman R (1991) Physical basis of cognitive alterations in Alzheimer's disease: synapse loss is the major correlate of cognitive impairment. Ann Neurol 30:572–580

Tomlinson BE, Blessed G, Roth M (1968) Observations on the brains of non-demented old people. J Neurol Sci 7:331–356

Toth M, Kiss A, Kosztolanyi P, Kondakor I (2007) Diurnal alterations of brain electrical activity in healthy adults: a LORETA study. Brain Topogr 20:63–76

Walsh DM, Klyubin I, Fadeeva JV, Cullen WK, Anwyl R, Wolfe MS, Rowan MJ, Selkoe DJ (2002) Naturally secreted oligomers of amyloid beta protein potently inhibit hippocampal long-term potentiation in vivo. Nature 416:535–539

Wang Z, Jia X, Liang P, Qi Z, Yang Y, Zhou W, Li K (2012) Changes in thalamus connectivity in mild cognitive impairment: evidence from resting state fMRI. Eur J Radiol 81:277–285

Williams VJ, Leritz EC, Shepel J, McGlinchey RE, Milberg WP, Rudolph JL, Lipsitz LA, Salat DH (2013) Interindividual variation in serum cholesterol is associated with regional white matter tissue integrity in older adults. Hum Brain Mapp 34:1826–1841

Wirth M, Oh H, Mormino EC, Markley C, Landau SM, Jagust WJ (2013) The effect of amyloid β on cognitive decline is modulated by neural integrity in cognitively normal elderly. Alzheimers Dement 9:687–698

Wood WG, Schroeder F, Avdulov NA, Chochina SV, Igbavboa U (1999) Recent advances in brain cholesterol dynamics: transport, domains, and Alzheimer's disease. Lipids 34:225–234

Xiong H, Callaghan D, Jones A, Walker DG, Lue LF, Beach TG, Sue LI, Woulfe J, Xu H, Stanimirovic DB, Zhang W (2008) Cholesterol retention in Alzheimer's brain is responsible for high beta- and gamma-secretase activities and Abeta production. Neurobiol Dis 29:422–437

Yesavage JA, BrinK TL, Rose TL, Lum O (1983) Development and validation of a geriatric depression scale: a preliminary report. J Psychiat Res 17:37–49

Yotter RA, Doshi J, Clark V, Sojkova J, Zhou Y, Wong DF, Ferrucci L, Resnick SM, Davatzikos C (2013) Memory decline shows stronger associations with estimated spatial patterns of amyloid deposition progression than total amyloid burden. Neurobiol Aging 34:2835–2842

Zhou B, Liu Y, Zhang Z, An N, Yao H, Wang P, Wang L, Zhang X, Jiang T (2013) Impaired functional connectivity of the thalamus in Alzheimer's disease and mild cognitive impairment: a resting-state FMRI study. Curr Alzheimer Res 10:754–766